

Analysis of the Shape of the T-wave in Congenital Long-QT Syndrome Type 3 by Geometric Morphometrics

Hitoshi Horigome

University of Tsukuba

Yasuhiro Ishikawa (✉ wavelet@nifty.ne.jp)

Ishikawa Medical Clinic, Saitama

Hirokazu Takahashi

Kizawa Memorial Hospital, Pediatrics

Masao Yoshinaga

Kagoshima Medical Center

Naokata Sumitomo

Saitama International Medical Center

Research Article

Keywords: long -QT syndrome type 3 (LQTS3), independent component (IC2), principal component (PC2)

Posted Date: January 21st, 2021

DOI: <https://doi.org/10.21203/rs.3.rs-148061/v1>

License: © ⓘ This work is licensed under a Creative Commons Attribution 4.0 International License.

[Read Full License](#)

Analysis of the shape of the T-wave in congenital long -QT syndrome type 3 by geometric morphometrics

Hitoshi Horigome¹⁺, Yasuhiro Ishikawa^{2*+}, Hirokazu Takahashi³, Masao Yoshinaga⁴, and Naokata Sumitomo⁵

¹Department of Child Health, Faculty of Medicine, University of Tsukuba, Tsukuba, Ibaraki, Japan

²Ishikawa Medical Clinic, Internal Medicine, Saitama, Japan

³Kizawa Memorial Hospital, Pediatrics, Minokamo, Gifu, Japan

⁴Department of Pediatrics, National Hospital Organization Kagoshima Medical Center, Kagoshima, Japan

⁵Department of Pediatric Cardiology, Saitama Medical University International Medical Center, Hidaka, Japan

*e-mail: wavelet@nifty.ne.jp

+The first and second authors contributed equally to this work

ABSTRACT

The characteristic shape of the T-wave in congenital long -QT syndrome type 3 (LQTS3) is considered a late-onset T-wave. We analyzed the difference in the shapes of T-waves between LQTS3 cases and normal subjects using generalized Procrustes analysis (GPA). The J and Q points of V5 in the ECGs of LQTS3 cases are shifted to the upper left compared to those of normal subjects. SdFmax is the point on the ECG where the second derivative is first maximized. The curvature of the T-wave takes the first maximum value at SdFmax where the T-wave has the smallest radius of curvature. The SdFmax in LQTS3 cases is shifted to the lower right compared to normal subjects. The interval from J to SdFmax of LQTS3 cases is expanded compared with that of normal subjects. As a result of principal component analysis (PCA) of the Procrustes mean shape of the T-wave landmarks, the second principal component (PC2) shows the shift in SdFmax to the lower right. These results can quantitatively explain why the T-wave of LQTS3 cases looks like a late-onset T-wave. Fitted to a multivariate logistic regression model, LQTS3 cases and normal subjects can be distinguished by the second independent component (IC2).

Introduction

Abnormalities in the shape of the T-wave as well as QT prolongation are often observed in congenital long -QT syndrome (LQTS). In recent years, it has been found that the cause of LQTS is abnormalities in the myocardial ion channels. Mutations in the ion channels have been shown to indicate the characteristic shape of T-waves to a certain degree^{1,2}. However, the classification of the shape of T-waves in LQTSs is subjective and intuitive. It has been difficult to say whether the shape of T-waves can be analyzed quantitatively up to the present. Recently, the method called “geometric morphometrics” or “statistical shape analysis” has been established as a tool for a quantitative analysis of the shape to settle the transformation and mutation of the creature. LQTS type 3 (LQTS3) has a third of the frequency compared to the 15 currently known forms of LQTS and a “late-onset T-wave” is said to be the feature for the shape of the T-wave of LQTS3. We analyzed the possibility of distinguishing LQTS3 subjects from normal subjects by the difference in the shapes of T-waves using methodology from statistical shape analysis³ (geometric morphometrics)^{4,5,6}. Initially, we need to describe the shape (in this paper, lead V5 of the ECG) by locating a finite number of points, called landmarks, on each specimen. A landmark is a point of correspondence on each object (lead V5 of the ECG) between and within populations.^{3,4} A two-dimensional curve (in this paper, the T-wave of V5) can be defined by the curvature of a curve (the Frenet-Serret formulas). The curvature can be calculated from the first and second derivatives as follows. If the plane curve is given in Cartesian coordinates as $y(x)$, then the curvature is $\kappa = y'' / (1 + y'^2)^{3/2}$, where $y' = dy/dx$, and $y'' = d^2y/dx^2$. When y' (the first derivative) is very small, κ can be approximated by y'' (the second derivative). Therefore, the points that take the maximum and minimum values of the first and second derivatives are considered important landmarks. Details will be explained in the results section, as shown in Figure 1, The following 9 landmarks were selected for in V5 of the ECG: the Q point, J point, the point where the curvature of the T-wave is maximized first (SdFmax), the point where the slope of the T-wave is maximized (FdFmax), the apex of the T-wave (Tp), the point where the slope of the T-wave is first minimized (FdFmin), the point where the curvature of the T-wave is maximized for the second time (SdSmax), the end point (Te) of T-wave by the tangent method and the end point of the T-wave identified

by the naked eye (TeEye).

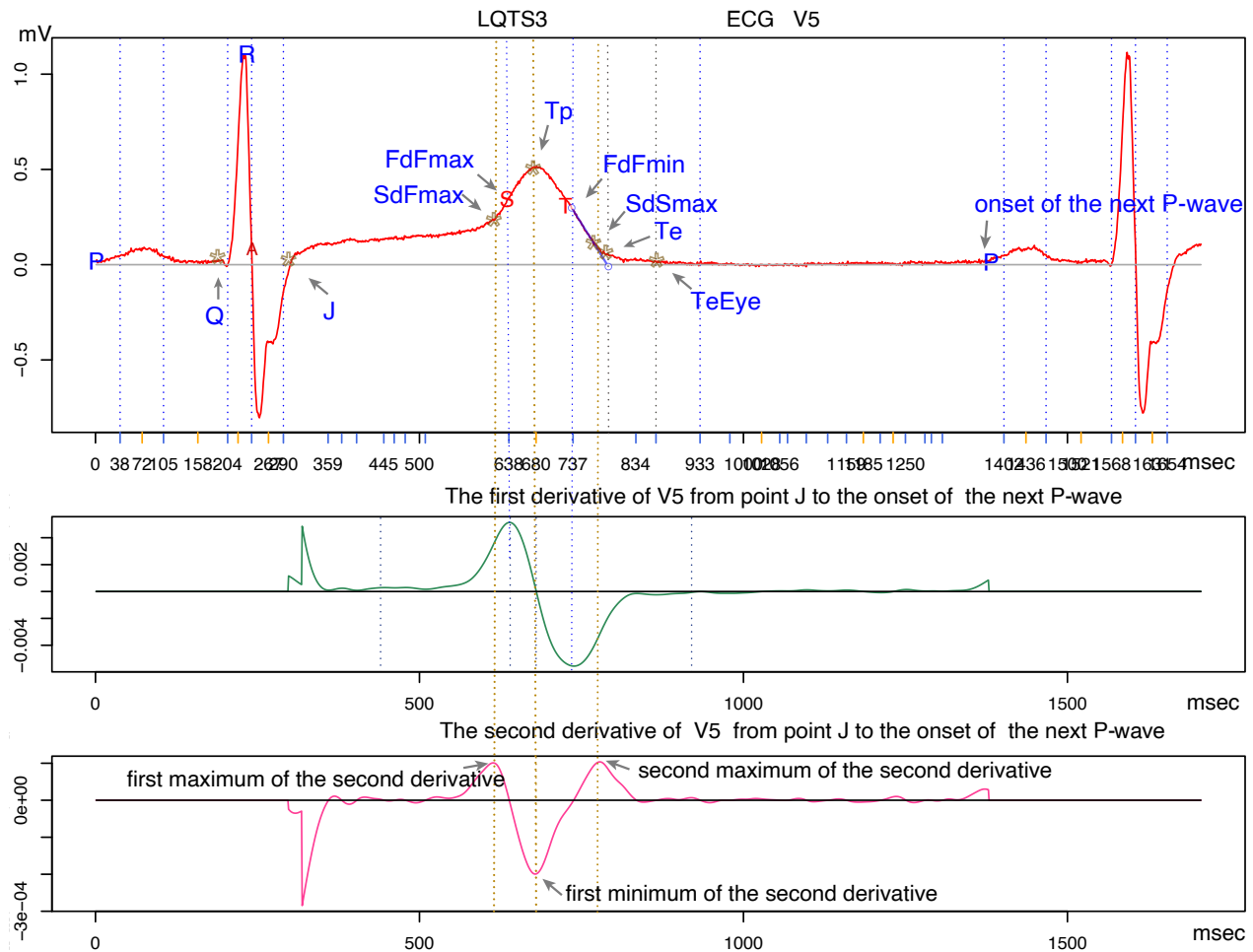


Figure 1. Top panel shows V5 of an ECG (red). The middle panel shows the first derivative (green). The bottom panel shows the second derivative (pink). Abbreviations are described in the text.

Result

Result of ECG measurement

Figure 2 shows violin plots for the comparisons of landmarks of the x-coordinates (SdFmax, FdFmax, Tp, FdFmin, SdSmax and Te) between the normal subjects and patients with LQTS3. The mean values of the x-coordinate landmarks were greater for the patients with LQTS3 than for the normal subjects. The p-values of the landmarks of x-coordinates are less than 0.001. The difference between the mean values of the two groups is statistically significant. The Bayes' factor⁷ values $\log_e(BF_{01})$ ⁸ are less than -12 . The Bayes' factors also show decisive evidence in favor of the null hypothesis.

The mean values of the y-coordinate landmarks were higher in the normal subjects than in the LQTS3 subjects, excluding Te (figure not shown.). The p-value of the y-coordinate of Te was 0.050011. The Bayes' factor of the y-coordinate of Te is not worth mentioning. The p-values of the other y-coordinate landmarks were less than 0.01. The Bayes' factor of the y-coordinate of SdFmax was -2.407 and was thought to be strong evidence in favor of the null hypothesis. The Bayes' factors of the other y-coordinate landmarks were between -2.05 and -1.66 and indicate substantial evidence.

Figure 3 shows the simply averaged shape from the data of 9 landmarks of 12 normal subjects (red) and 12 LQTS3 cases (green) without translation, rescaling or rotation. Q is zero at the starting point. The x-coordinates of the landmarks were corrected using the Bazett formula. Abbreviations in the figure are defined in the main text of this paper. The 95% confidence interval for J and TeEye are indicated by a blue solid horizontal line. Dashed ovals indicates the 95% confidence ellipses⁴ for

the other landmarks. The red 95% confidence ellipses are for the normal subjects, and the green ellipses are for the patients with LQTS3. The 95% confidence ellipses of the landmark in the normal subjects and that of the corresponding landmark in the patients with LQTS3 did not overlap. The 95% confidence ellipse of SdFmax in the normal subjects is vertically long, but that in the patients with LQTS3 is exceptionally horizontally long. However, the 95% confidence ellipses of FdFmax, Tp and FdFmin of the two groups are vertically long.

Generalised Procrustes analysis results

Generalized Procrustes analysis (GPA) was carried out in the shapes R package⁹. GPA is a method involving translating, rescaling and rotating the configurations relative to each other to minimize a total sum of squares⁹. Panel **a** of Figure 4 shows the mean shape of the T-wave for the normal subjects (red) registered to the mean shape of the T-wave for the patients with LQTS3 (green) registered by full GPA. The curvature of the T-wave is maximized at the first local maximum of the second derivative (SdFmax). SdFmax is the first point where the T-wave has the smallest radius of curvature and the largest bend. The SdFmax of the patients with LQTS3 (green) was slightly displaced to the lower right compared with that of the normal subjects (red). The interval from *J* to SdFmax of the patients with LQTS3 (green) was expanding compared with that of normal subjects (red). The slope of the ascending limb of the T-wave is maximized at first local maximum of the first derivative (FdFmax). Both FdFmax and Tp (the peak of the T-wave) for the patients with LQTS3 (green) were pulled downward. The displacements of these x-coordinates were only slightly to the right. The amplitudes of the patients with LQTS3 were smaller than those of the normal subjects. FdFmin is the coordinate the slope of the descending limb of the T-wave is minimized. There was not much difference between LQTS3 (FdFmin) and normal subjects. SdSmax is the coordinate of V5 at which the second derivative obtains the local maximum of the second time. The curvature of the descending limb of the T-wave is the maximum at this point. The SdSmax of the patients with LQTS3 (green) was pulled to the right upward slightly compared with that of normal subjects (red). Both Te and TeEye for the patients with LQTS3 show displacement toward the upper right. Compared with the normal subjects, it was observed that the distance between *J* and SdFmax increased and the amplitude of the T-wave decreased in the patients with LQTS3. Panel **b** of Figure 4 shows a thin-plate spline transformation grid to minimize mixed energy from the normal subject mean (red) to the LQTS3 mean (green). A blue arrow is drawn from the normal subjects' mean shape (red) to the mean shape of the patients with LQTS3 (green). The shape change has not been magnified. The space from *J* to SdFmax is stretched. The space near the apex of the T-wave is pushed downward and the space near the end point of the T-wave is displaced upward.

Test for the mean shape difference

Goodall's F test⁹ for mean shape differences, including permutation and bootstrap tests, was performed between 12 normal subjects and 12 patients with LQTS3. From the output of Goodall's F test for two independent samples, the tabular p-value = 0, the permutation p-value (10000 iterations) is 0.0004 and the bootstrap p-value (10000 iterations) is 0.0003. There was a significant difference between the mean shape of the normal subjects and the mean shape of the patients with LQTS3 from Goodall's F test.

Results of the shape PCA and ICA

GPA was performed on the landmarks of the normal subjects alone, the landmarks of the patient with LQTS3 alone and the combination of the two types (normal subjects and patient with LQTS3). Figure 5 displays a change in the principle components of the normal subjects alone (panels **a**, and **b**), the patient with LQTS3 alone (panels **c** and **d**) and the combination of the data (panels **e** and **f**). The left column of Figure 5 shows PC1 and the right column of Figure 5 shows PC2. A square grid is drawn around the mean shape (red points) and deformed using a pair of thin-plate splines to an icon (green points, $c = 1 * \text{standard deviations}$) along each PC (indicated by a blue vector from the mean to the icon). Each PC1 of the normal subjects (panel **a**) and the patients with LQTS3 (panel **c**) shows *Q*, *J*, SdSmax, Te and TeEye were attracted to the vertical center line and narrowed. FdFmax and Tp is displaced upward. Each SdFmax of PC2 of the normal subjects (panel **b**) and the patients with LQTS3 (panel **d**) is displaced to the upper left. In the case of the combination of the two types (the normal subjects and the patients with LQTS3), PC1 (panel **e**) for the Procrustes mean shape shows the displacement to the left of *Q* and *J*. FdFmax and Tp were displaced downward. Te, SdSmax and TeEye were pulled to the upper right. There are almost no changes in SdFmax and FdFmin. PC2 (panel **f**) for the the Procrustes mean shape shows the displacement to the lower right of SdFmax. The orientation of the vector of SdFmax is the opposite of that of SdFmax in panels **b** and **d**. We see that the percentage of variability explained by the first two PCs is 89.4% (panel **e**) and 5.3% (panel **f**). The PCA result shows that *s* (the centroid size, the centroid size is the square root of the sum of squared Euclidian distances from each landmark to the centroid.^{3,9}) and PC1 give reasonably good separation of the two groups (figure not shown). As a further indication, we considered ICA, which seeks the most non-Gaussian directions of variability. There are many types of ICAs and we use JADE which is available in R.¹⁰ Figure 6 shows plots of the independent component (IC) scores and PC scores for the T-wave

landmark data. We see that IC2 gives quite good separation between the normal subjects and the patients with LQTS3. Red numbers indicate normal subjects, and blue numbers indicate patients with LQTS3.

Multivariate logistic regression modeling

Multivariate logistic regression model selection was carried out in the `bestglm` R package¹¹. Logistic regression is a method for fitting a regression curve, $y = f(x)$, when y is a categorical variable (in this paper, normal subjects or patients with LQTS3). The typical use of this model is predicting y given a set of predictors (explanatory variables) x . As the objective (response) variable, $normal\ subjects = 1$, and $LQTS3 = 0$. Using five explanatory variables (the centroid size s , Riemannian distance ρ ^{3,9,12} to the mean shape and the first three PC scores. Riemannian distance ρ is the geodesic distance between individual specimens and mean shape in Kendall's shape space¹².), we fitted a multivariate logistic regression model for these data. For all combinations of the five explanatory variables, variable selection was performed by minimizing Akaike's information criterion (AIC). $p = (\exp(689.8 - 995.3 * s - 1307.2 * PC1)) / (1 + \exp(689.8 - 995.3 * s - 1307.2 * PC1))$ was adopted as the best model (AIC=6). In this equation, normal subjects and patients with LQTS3 can be completely distinguished (figure not shown.). Using five explanatory variables (the centroid size s , Riemannian distance ρ to the mean shape and the first three IC scores), we fit a multivariate logistic regression model for these data. For all combinations of the 5 explanatory variables, variable selection was performed with AIC minimization as a guide. $p = (\exp(72.91 + 748.09 * IC2)) / (1 + \exp(72.91 + 748.09 * IC2))$ was adopted as the best model (AIC=4). Based on the AIC, this expression is best model. In this equation, normal subjects and patients with LQTS3 can be completely distinguished.

Discussion

The LQTS3 model¹³ was induced by sea anemone toxin, a Na⁺ channel inactivation blocker. It prolonged the epicardial, M cell, and endocardial action potential durations (APDs) by prolonging phase 2, producing a long-ST segment, late-onset T-wave, and a markedly prolonged QT interval. LQTS3 was intuitively classified as 53% late-onset T-waves, 12% asymmetric T-waves, and 33% overlapping the long-QT type 1 pattern². In Figure 3, the 95% confidence ellipse of SdFmax in normal subjects is vertically long, but the 95% confidence ellipse of SdFmax in the patients with LQTS3 is exceptionally horizontally long, suggesting that LQTS3 may contain several patterns others than late-onset T-waves. We analyzed the possibility of distinguishing LQTS3 subjects from normal subjects by the difference in the shapes of the T-waves using methodology from statistical shape analysis, specifically GPA. There are more Q and J points in the upper left in the patients with LQTS3 than in the normal subjects. SdFmax which is the point at which the curvature of the T-wave is first maximized, of the patients with LQTS3 is slightly displaced to the lower right compared to that of the normal subjects. The interval from J to SdFmax of LQTS3 subjects is expanding compared with that of the normal subjects. These two results suggest that the rising point of the T-wave of the patients with LQTS3 is later than that of the normal subjects and looks like a "late-onset T-wave". The shape PCA of the T-wave landmark data shows that the displacement of Q and J to the left and the displacement of Te and $TeEye$ to the right were observed on PC1 (Figure 5, panel e). There are almost no changes in SdFmax and FdFmin. The second PC for the Procrustes mean shape shows displacement to the lower right for SdFmax (Figure 5, panel f). These results also suggest that the "late-onset T-wave" is the feature for the shape of the T-wave of patients with LQTS3. Shape PCA and ICA were performed to discriminate between patients with LQTS3 and normal subjects. Multivariate logistic regression model selection was carried out to discriminate between normal subjects and patients with LQTS3. We see that s (the centroid size) and PC1 give reasonably good separation of the two groups. We see that IC2 gives better separation than the PCA results. The fitted multivariate logistic regression model for our data, $p = (\exp(72.91 + 748.09 * IC2)) / (1 + \exp(72.91 + 748.09 * IC2))$ has been adopted as the best model (AIC=4). In this equation, normal subjects and patients with LQTS3 can be completely separated.

Methods

Subjects

We studied 12 patients (17.2 ± 13.3 years old, 7 males, 5 females) with genetically confirmed LQTS3 (by E1784k gene mutation) and 12 age-matched healthy control subjects free from cardiovascular diseases and medications with electrophysiological effects. The study protocol was approved by the Ethics Committee of the University Hospital of Tsukuba (Ibaraki, Japan), and informed consent was obtained from each patient or his or her parents if the patient was < 18 years old.

ECG data sampling

The ECGs were recorded as time series data using an ECG amplifier (Polymate AP1532; TEAC; Tokyo). The time constant was set at 3.0 seconds. Signals were recorded from 10 channels using 20 silver-chloride surface electrodes. Channel 1 was set as lead I; channel 2 was set as lead II; channel 3 was set as lead III; channels 4 to 9 were set as bipolar leads from the chest to the left leg, each corresponding to C1 to C6 of conventional 12-lead ECG; and channel 10 was set as 4C9, representing

a bipolar lead from the fourth intercostal space on the left spine border of the back to the fourth intercostal space at the left sternal border of the forechest. In each subject, the recorded data were digitized online with an A/D converter (EC-2360; Elmec; Tokyo, Japan) at a sampling rate of 2,048 Hz and saved in a notebook computer as a data file for future analysis. The data of C1 to C6 were converted into V1 to V6 using the following formula to produce ECG images: $V_i = C_i(II + III)/3$, where $i = 1, \dots, 6$ ^{14,15}. Two-dimensional curves can be defined by the curvature (the Frenet-Serret formula). Considering that the curvature can be calculated by the first derivative and the second derivative, the following 9 landmarks were measured with R language software for 10 consecutive beats in each ECG. As shown in Figure 1, the top panel shows V5 of the ECG. The middle panel shows the first derivative. The bottom panel shows the second derivative from point J to the next start point of the P-wave. We chose the following nine points in V5 as a landmark. The mean of each landmark for each case was analyzed.

1. The start point of the Q-wave, Q is $(x, y) = (0, 0)$.
2. The coordinates of point J are J , and the starting point of J is Q . In the following, a starting point is Q .
3. The coordinates of V5 where the first local maximum of the second derivative occurs (SdFmax).
4. The coordinates of V5 where the first local maximum of the first derivative occurs (FdFmax).
5. The coordinates of the peak of the T-wave (T_p). At this x-coordinate, the second derivative takes the first minimum value.
6. The coordinates of V5 where the first local minimum of the first derivative occurs (FdFmin).
7. The coordinates of V5 where the second local maximum of the second derivative occurs (SdSmax).
8. The x-coordinate indicates that a tangent from the FdFmin point crosses a baseline (T_{end}), and the y-coordinate indicates the T_{end} of V5 (T_e).
9. The visual end of the T-wave, $y = 0$ (T_{eEye}).

The x-coordinate from the distance of Q is revised via Bazett correction. The y-coordinate is not revised.

Measuring method of the ECG

In the original R program, the top panel of Figure 1 (V5 of the ECG) is first displayed. The Q point (Q), J point (J) and visual T-wave end-point (T_{eEye}) were determined by selecting the points with the naked eye and clicking the mouse. The first derivative of V5 was obtained by applying a smoothing spline to the difference in V5. The second derivative of V5 was obtained by applying a smoothing spline to the difference in this first derivative. When the local maxima and minima of the first and second derivatives are found, it is possible to determine the abovementioned coordinates. The coordinate of SdFmax was obtained as the point where the vertical orange dashed line from the x-coordinate of the first maximum of the second derivative intersects V5 on the top panel of Figure 1. FdFmax can be determined by clicking the mouse the point (S) where the blue dotted vertical line drawn from the x-coordinate of the first maximum of the first derivative intersects the ascending limb of the T-wave on the top panel. The coordinates of FdFmin were obtained by the vertical line of the blue dotted line drawn from the x-coordinate of the minimum value of the first derivative of the middle panel as the intersection with the descending limb of the T-wave of the top panel of Figure 1. The x-coordinate of the endpoint of the T-wave by the tangent method (T_e) is calculated as a point at which a tangent from point T (FdFmin) crosses a baseline. The x-coordinate of SdSmax (the second local maximum of the second derivative) was obtained by calculating the maximum of the second derivative between FdFmin and T_{eEye} .

Analysis

The most common types of statistical tests, namely, parametric, nonparametric and robust tests, and Bayesian versions of the t-test/ANOVA were carried out in the ggstatsplot R package⁸. GPA was carried out in the shapes R package⁹. GPA is a method to register landmark configurations optimally using translation, rotation and scaling. Goodall's F test⁹ for mean shape differences, including permutation and bootstrap tests was performed between the 12 normal subjects and the 12 patients with LQTS3. ICA was carried out in the ica R package¹⁰. Multivariate logistic regression model selection was carried out with the bestglm R package¹¹.

All methods were carried out in accordance with relevant guidelines and regulations.

Acknowledgements

This work was partly supported by a Health and Labour Sciences Research Grant from the Ministry of Health, Labour and Welfare of Japan (H29-055).

Author Contributions

H.H.,Y.I. and H.T. conceived the study and performed statistical analyses. H.H.,H.T.,M.Y. and N.S. acquired the data. H.H. and Y.I. wrote the paper. All authors reviewed the manuscript and provided meaningful intellectual contributions.

Conflicts of Interest

The authors declare that there are no conflicts of interest.

References

1. Moss AJ. et al. ECG T-wave patterns in genetically distinct forms of the hereditary long -QT syndrome. *Circulation*. 92,2929-2934(1995).
2. Zhang L. et al. Spectrum of ST-T-wave patterns and repolarization parameters in congenital long -QT syndrome: ECG findings identify genotypes. *Circulation*.102,2849-2855(2000).
3. Dryden I.L.,Mardia K.V. *Statistical Shape Analysis with Applications in R*. 2nd ed:(Chichester:Wiley;2016).
4. Claude J. *Morphometrics with R*. (New York:Springer,2008).
5. Zelditch M.L.,Swiderski D.L.,Sheets H.D. *Geometrics Morphometrics for Biologists*. 2nd ed: (London:Elsevier,2012).
6. Bookstein F.L. *Morphometric Tools for Landmark Data Geometry and Biology*. (Cambridge:Cambridge University Press,1997).
7. Harold J. *The Theory of Probability* . (Oxford: England ,1961).
8. Patil, I. ggstatsplot: "ggplot2" Based Plots with Statistical Details. CRAN. Retrieved from <https://CRAN.R-project.org/package=ggstatsplot> (2020).
9. Dryden I.L. shapes: Statistical Shape Analysis. R package version 1.2.0. <https://CRAN.R-project.org/package=shapes> (2017).
10. Helwig N.E. ica: Independent Component Analysis. R package version 1.0-1. <https://CRAN.R-project.org/package=ica> (2015).
11. McLeod A.I., Xu C. bestglm: Best Subset GLM and Regression Utilities. R package version 0.37. <https://CRAN.R-project.org/package=bestglm> (2018).
12. Kendall, D. G. Shape manifolds, Procrustean metrics and complex projective spaces, *Bulletin of the London Mathematical Society*, 16, 81-121(1984).
13. Wataru S, Chales A. Sodium channel block with mexiletine is effective in reducing dispersion of repolarization and preventing torsade de pointes in LQT2 and LQT3 models of the long -QT syndrome. *Circulation*.96,2038–2047(1997).
14. Hitoshi H. et al.Multivariate analysis of TU wave complex on electrocardiogram in Andersen–Tawil syndrome with KCNJ2 mutations.*Ann Noninvasive Electrocardiol*.25,186-194(2020)
15. Hitoshi H. et al. Detection of extra components of T-wave by independent component analysis in congenital long- QT syndrome. *Circulation. Arrhythmia and Electrophysiology*. 4, 456– 464(2011)

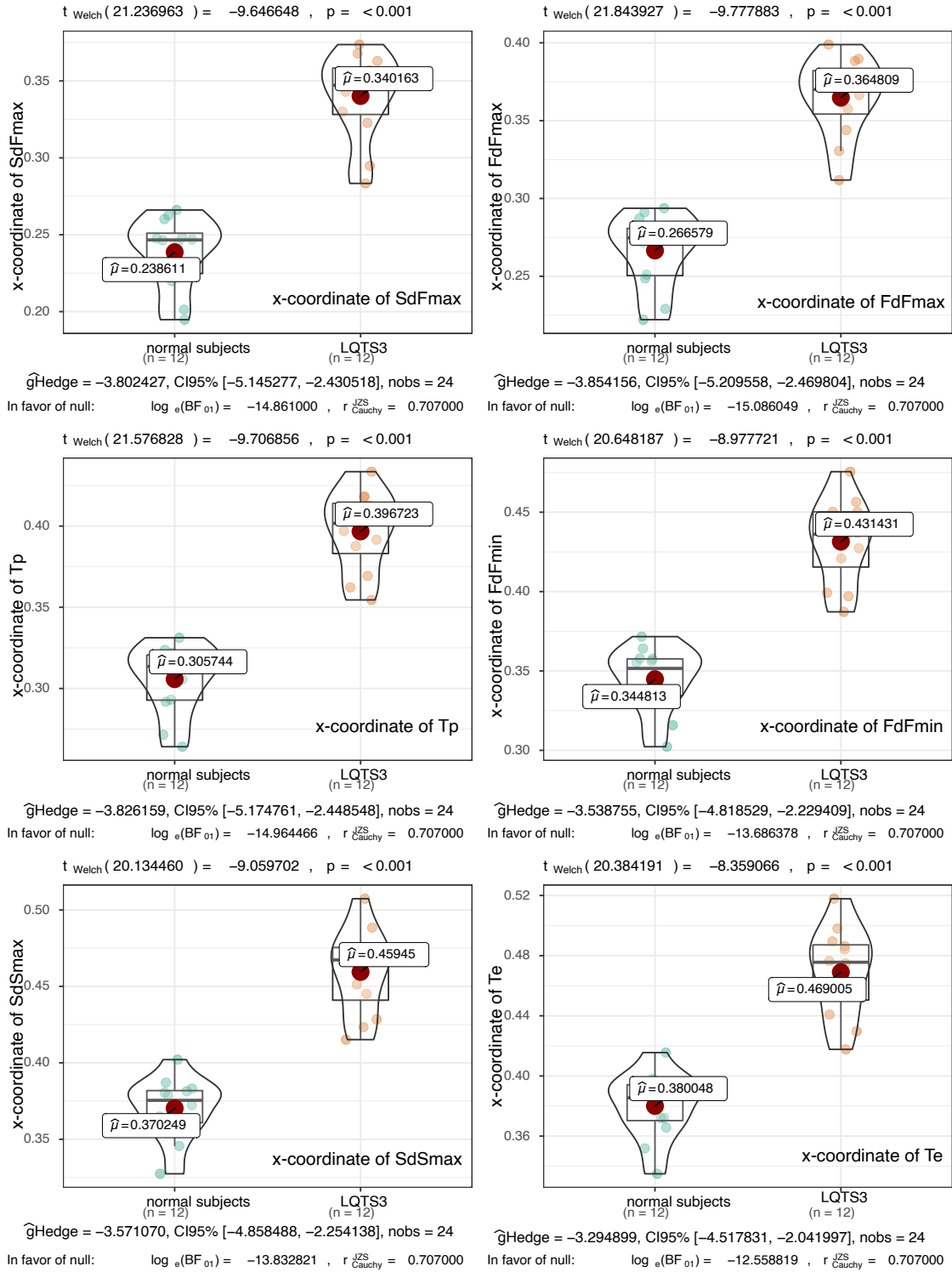


Figure 2. Violin plots for the comparisons of the landmarks of the x-coordinates (SdFmax, FdFmax, Tp, FdFmin, SdSmax and Te) between the normal subjects and the patients with LQTS3. The mean values of the x-coordinate landmarks were greater in the patients with LQTS3 than in the normal subjects. The P-values of the landmarks of x-coordinates are less than 0.001. Each Bayes' factors shows decisive evidence in favor of the null hypothesis.

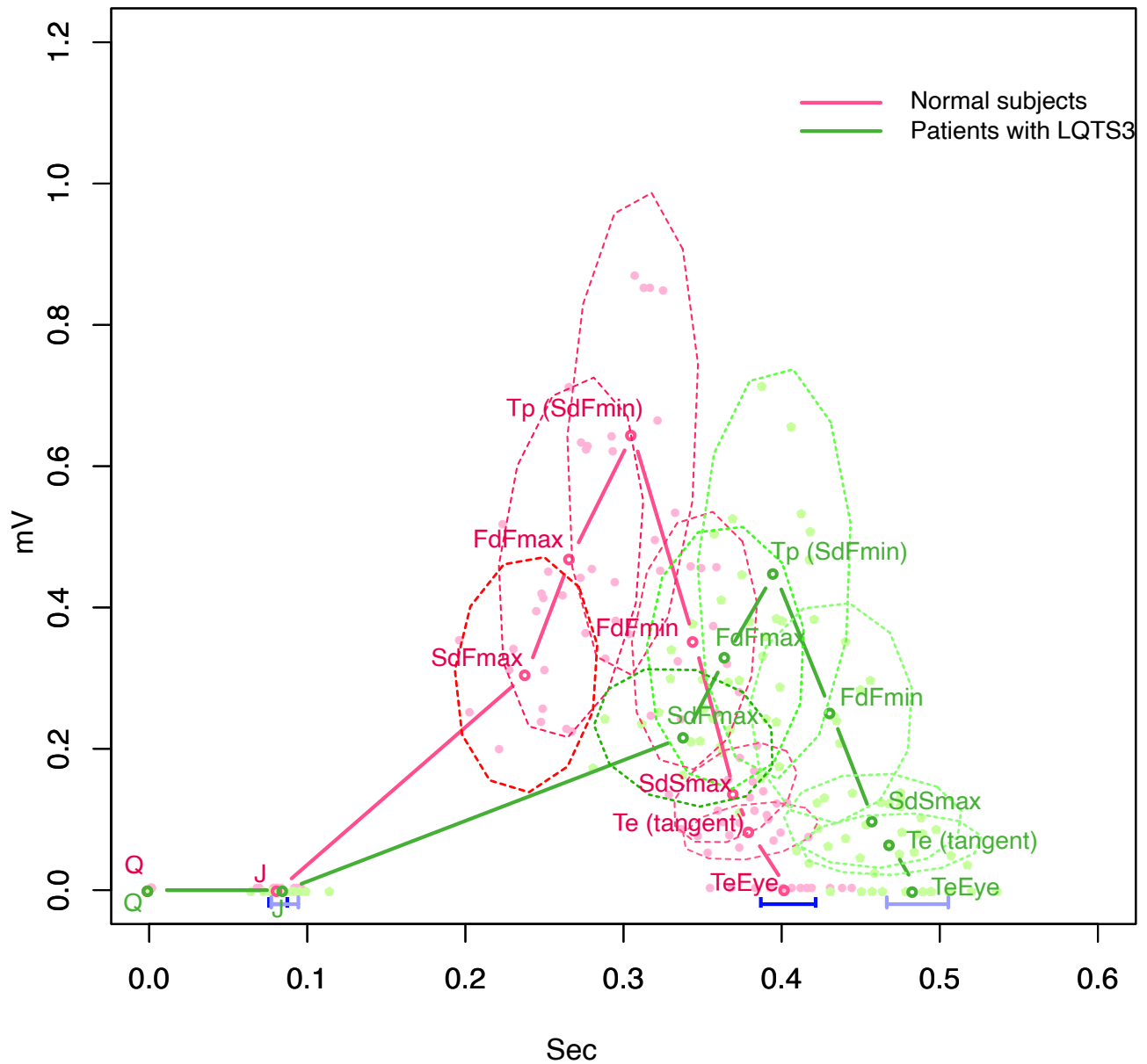


Figure 3. Simply averaged shape of 9 landmarks of the 12 normal subjects (red) and 12 LQTS3 (green) cases. Q is zero at the starting point. The x-coordinates of landmarks were revised by Bazett correction. The abbreviations in the figure are defined in the main text of this paper. The 95% confidence intervals of the J point and TeEye are indicated by blue solid horizontal lines. The dashed ovals indicate the 95% confidence ellipses for the other landmarks. The corresponding 95% confidence ellipses for landmarks do not overlap with each other. The pale pink dots are the landmarks of normal subjects, and the pale green dots are landmarks of the patients with LQTS3.

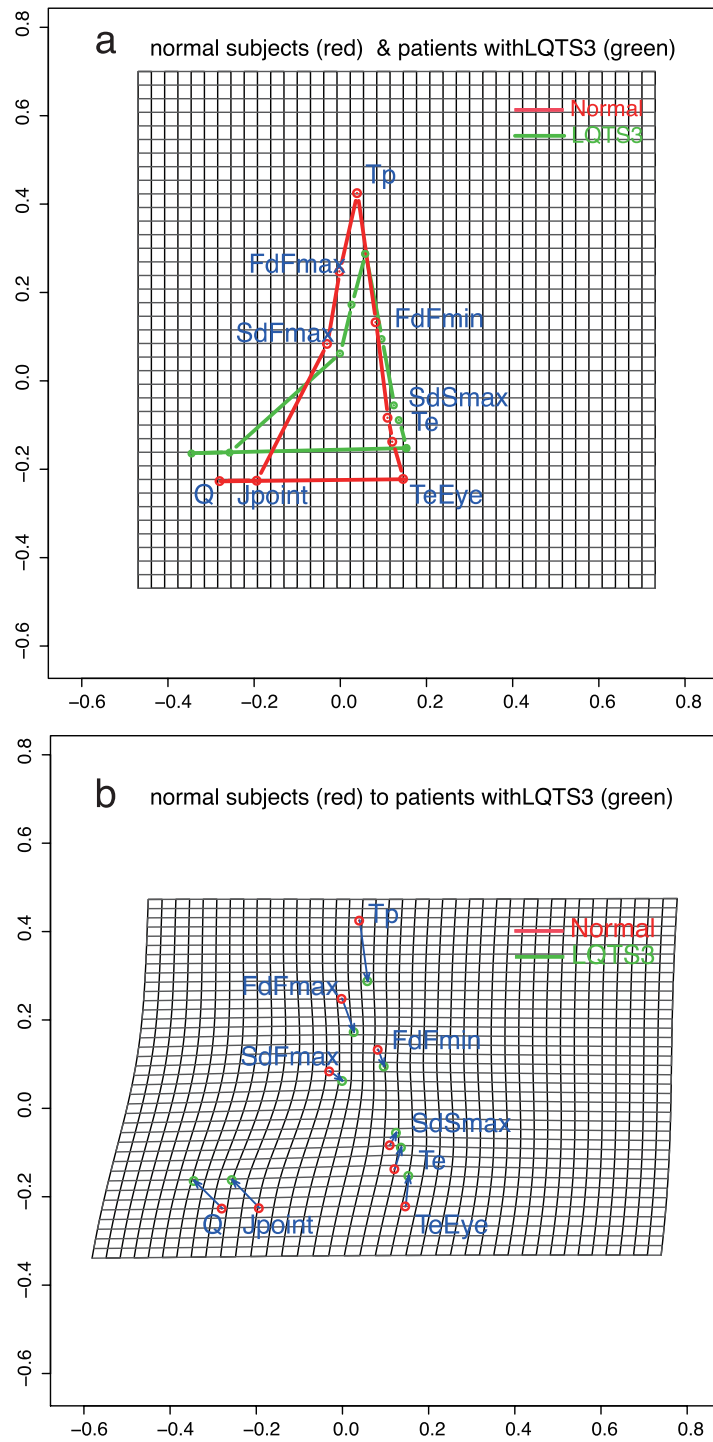


Figure 4. Panel **a** shows the mean shape of the T-wave in the normal subjects (red) and the mean shape of the T-wave in the patients with LQTS3 (green) by full GPA. Panel **b** shows thin-plate spline transformation grids to minimize the mixed energy from the normal mean shape (red) to the patients with LQTS3 mean shape (green), with blue arrows drawn from the normal subjects mean (red) to the patients with LQTS3 (green). The shape changes have not been magnified.

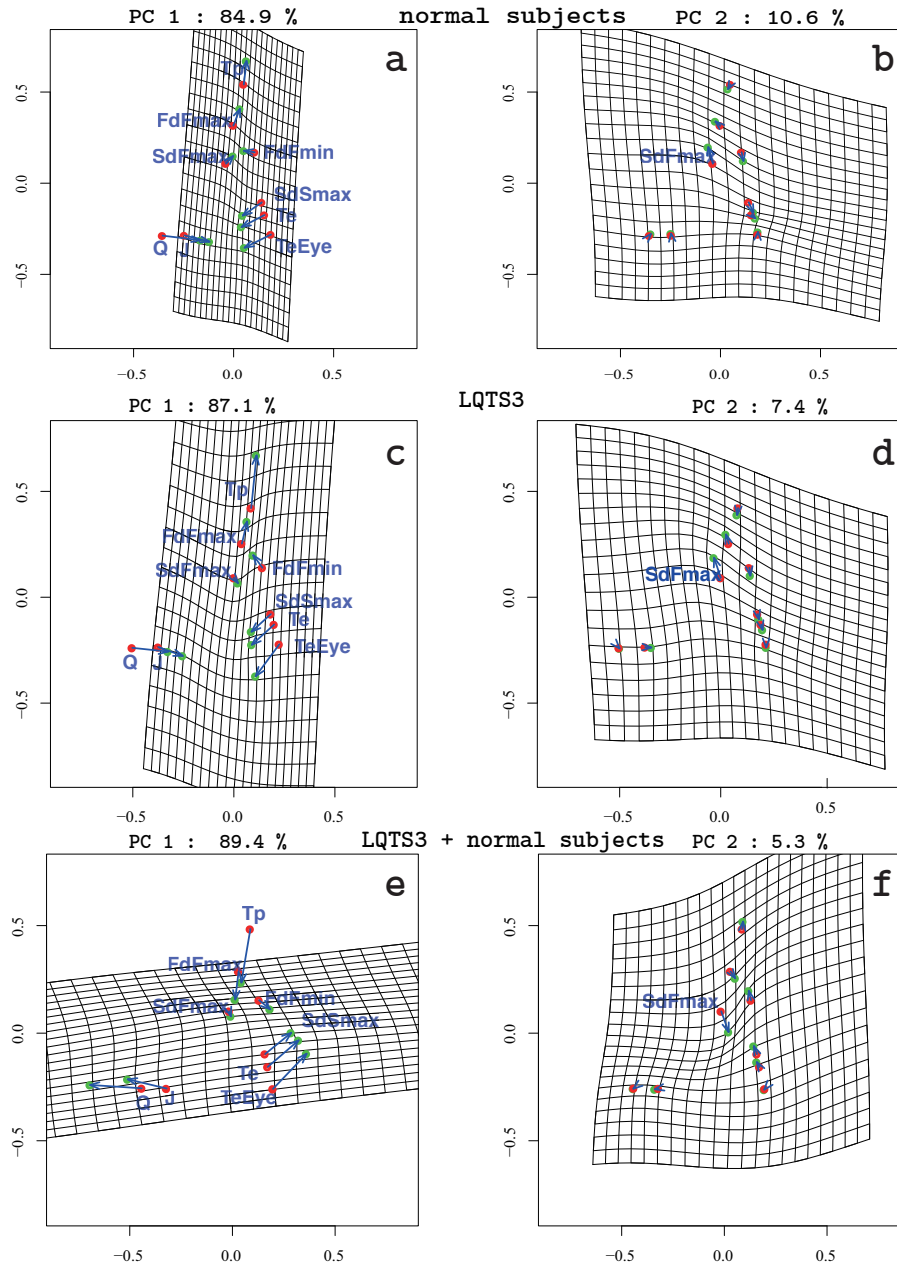


Figure 5. Changes in PC1 and PC2 in the normal subjects (panels **a** and **b**), patients with LQTS3 (panels **c** and **d**) and a combination of the two groups of subjects (panels **e** and **f**). A square grid is drawn on the mean shape (red points) and deformed using a pair of thin-plate splines to an icon (green points, *mean* + 1 * *standard deviation*) along each PC (indicated by the blue vector from the mean to the icon). PC1 of the normal subjects (panel **a**) and PC1 of the patients of LQTS3 (panel **c**) show that *Q*, *J*, *SdSmax*, *Te* and *TeEye* are attracted to the vertical center and narrowed. *FdFmax* and *Tp* are displaced upward. The *SdFmax* of PC2 of the normal subjects (panel **b**) and that of the patients with LQTS3 (panel **d**) is displaced to the upper left. In the case of the combination of the two types, PC1 (panel **e**) for the Procrustes mean shape shows the displacement to the left of *Q* and *J*. *FdFmax* and *Tp* were displaced downward. *SdSmax*, *Te*, and *TeEye* were pulled to the upper right. There are almost no changes in *SdFmax* and *FdFmin*. PC2 (panel **f**) for the Procrustes mean shape shows the displacement of *SdFmax* to the lower right.

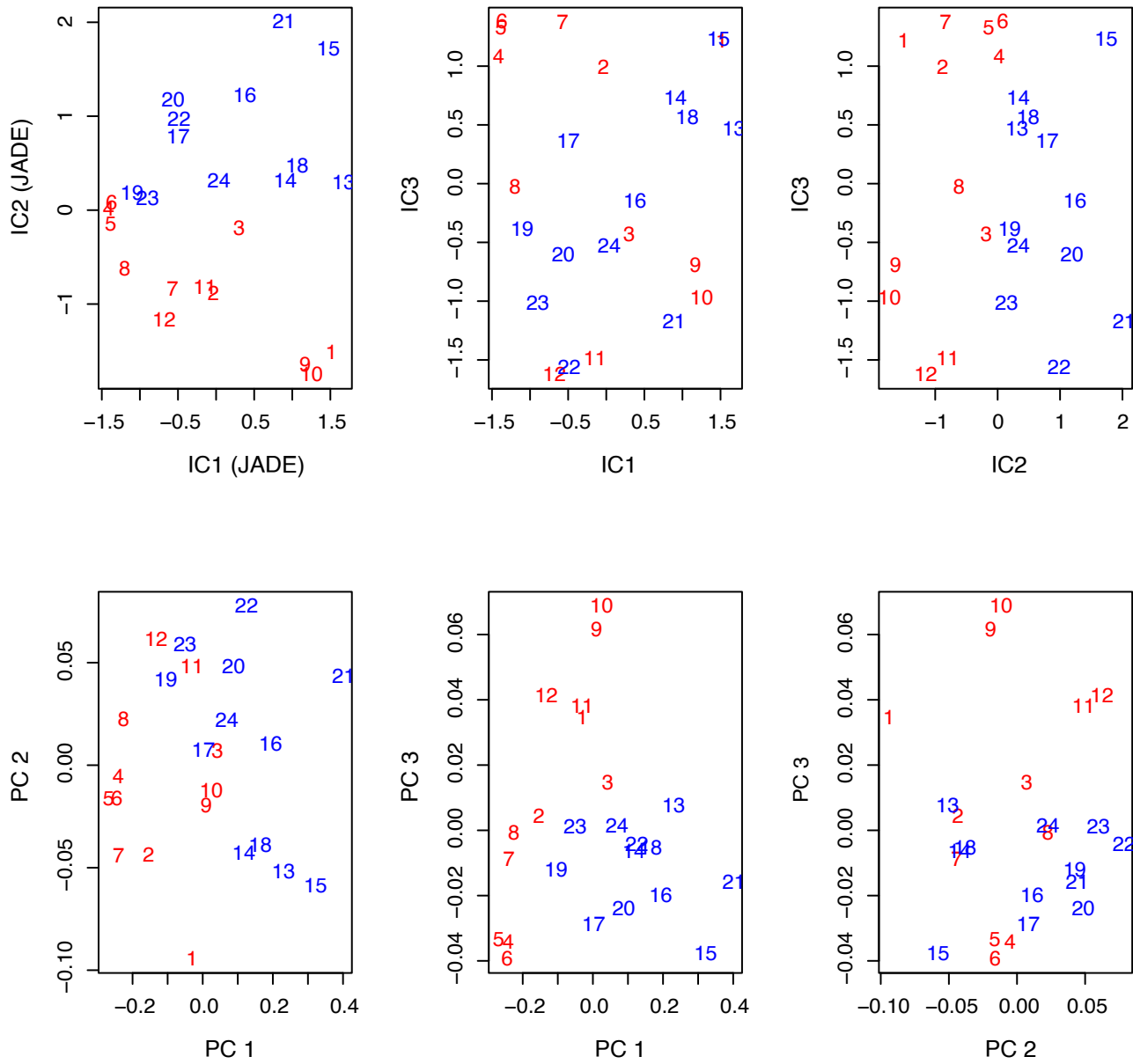


Figure 6. Plot of the first three IC scores(top row), and the first three PC scores (bottom row) for a combination of the landmark data. Red numbers indicate normal subjects, and blue numbers indicate patients with LQTS3. IC2 gives quite good separation between normal subjects and patients with LQTS3.

Figures

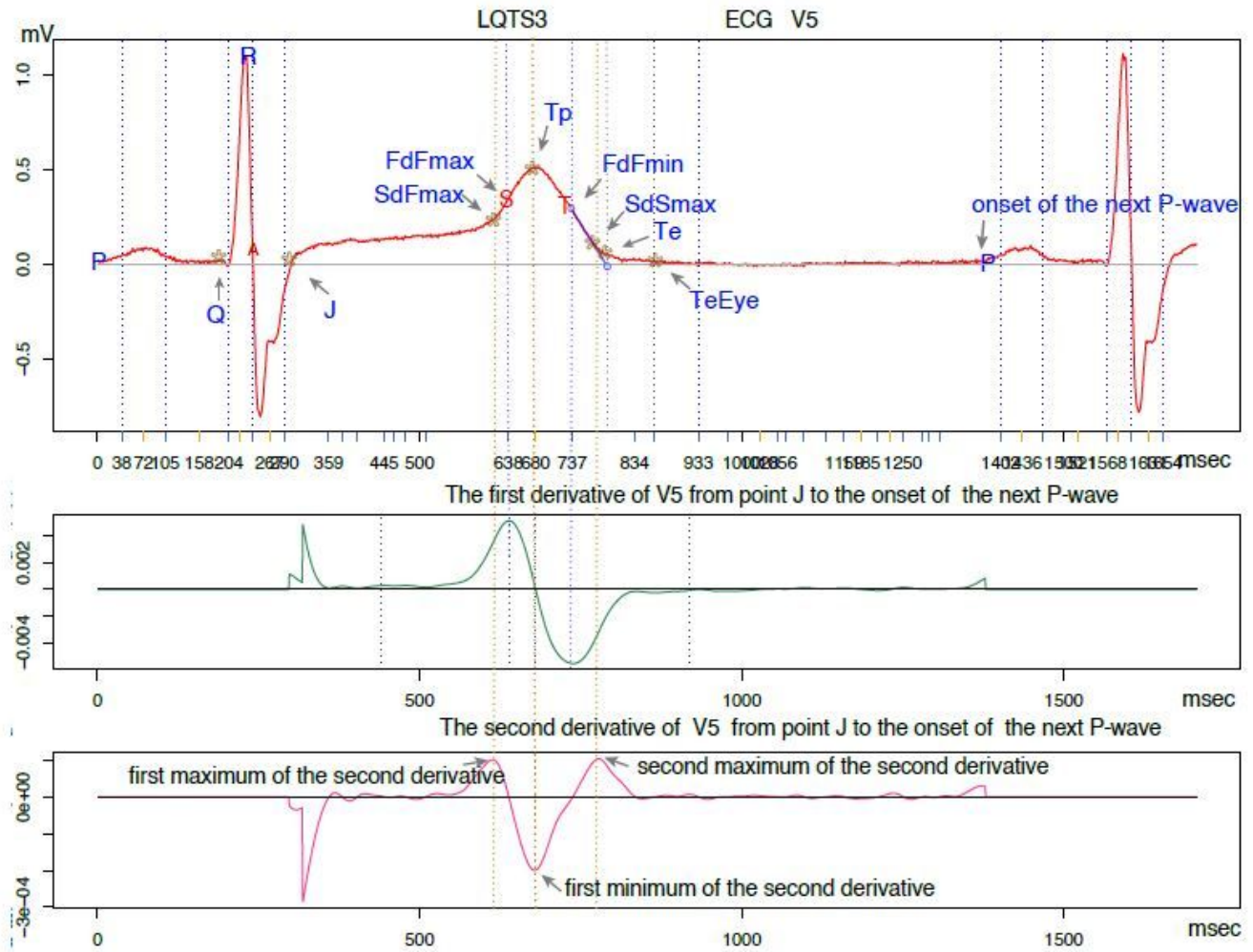


Figure 1

Top panel shows V5 of an ECG (red). The middle panel shows the first derivative (green). The bottom panel shows the second derivative (pink). Abbreviations are described in the text.

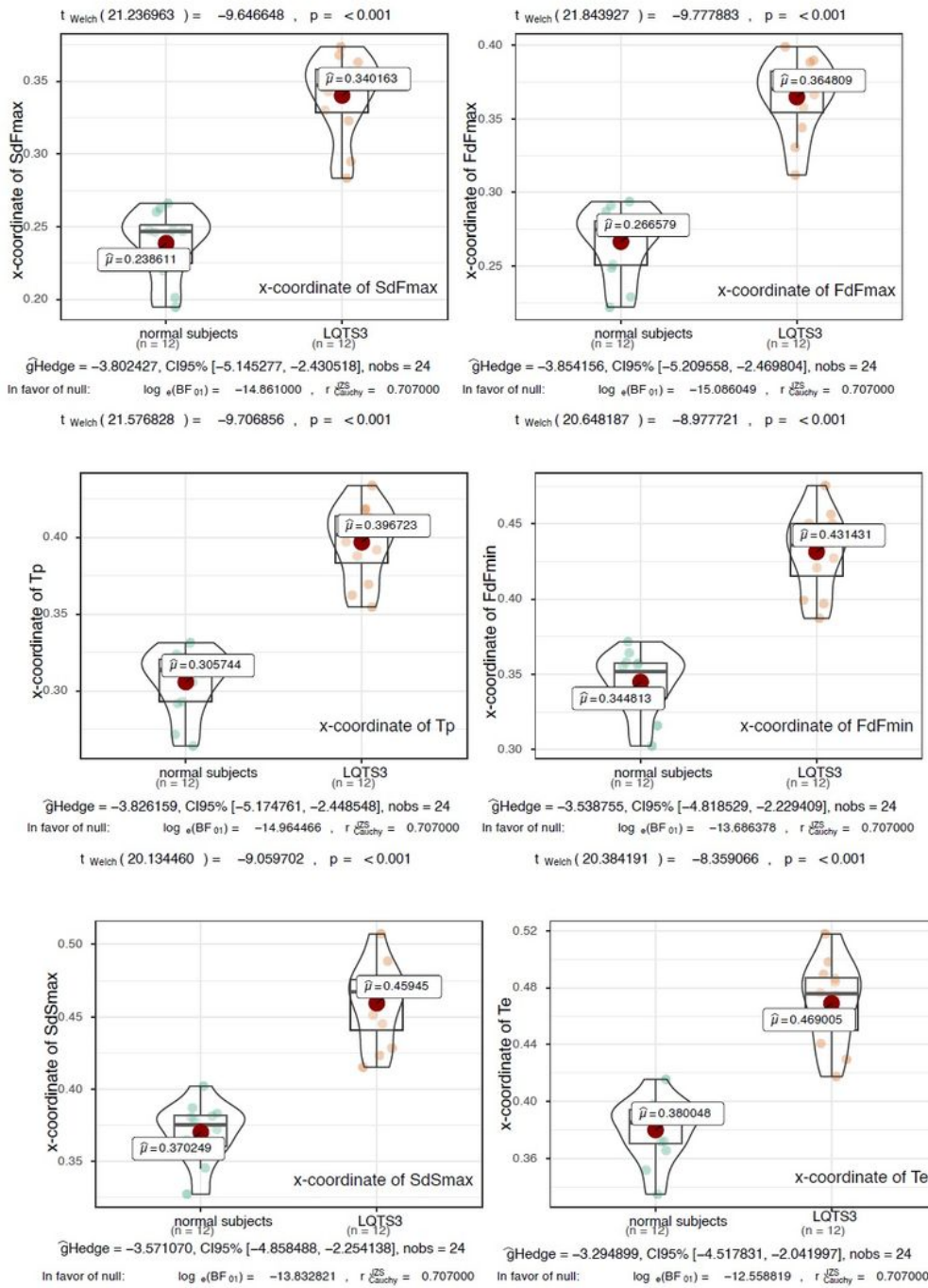


Figure 2

Violin plots for the comparisons of the landmarks of the x-coordinates (SdFmax, FdFmax, Tp, FdFmin, SdSmax and Te) between the normal subjects and the patients with LQTS3. The mean values of the x-coordinate landmarks were greater in the patients with LQTS3 than in the normal subjects. The P-values of the landmarks of x-coordinates are less than 0.001. Each Bayes' factors shows decisive evidence in favor of the null hypothesis.

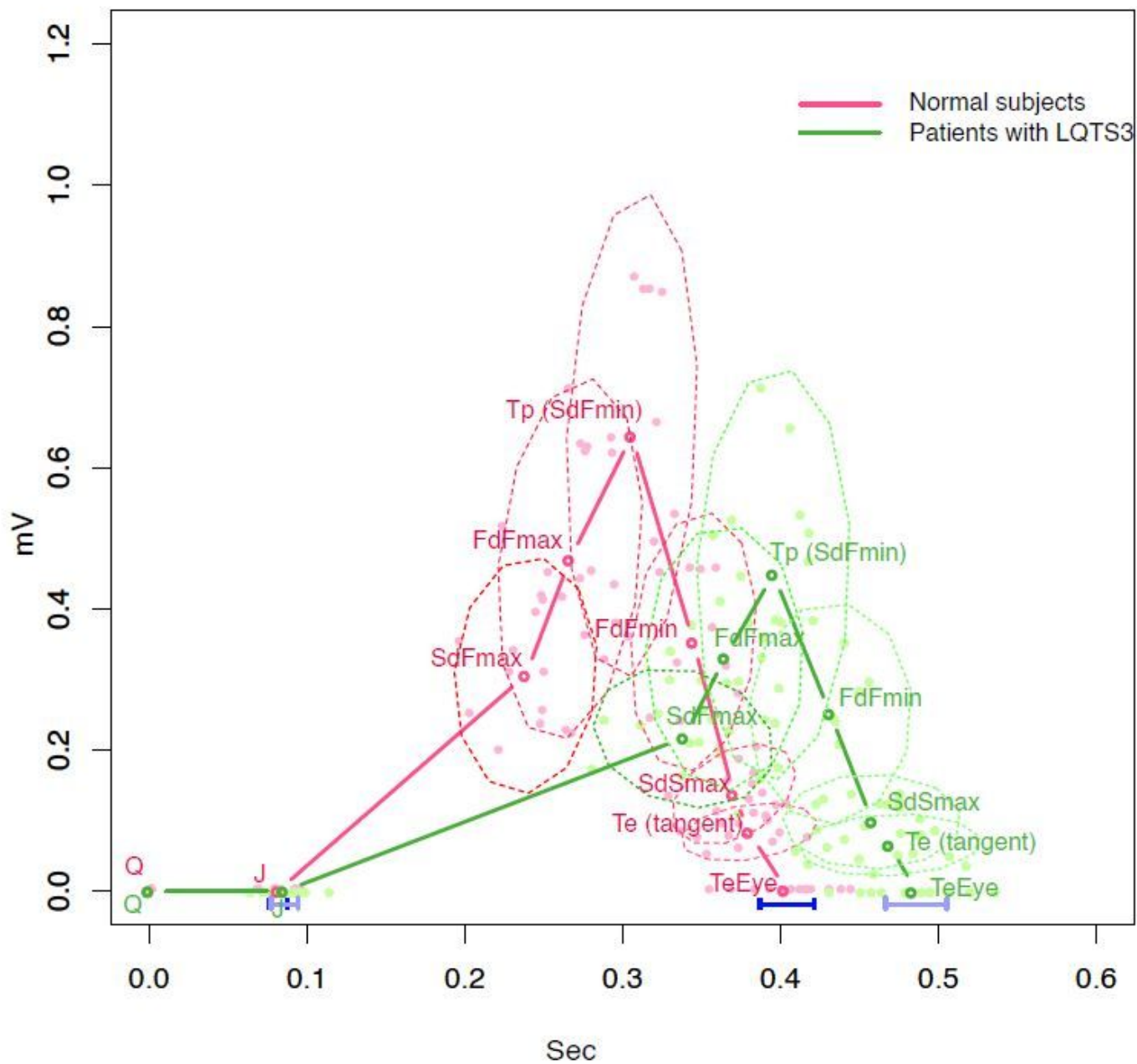


Figure 3

Simply averaged shape of 9 landmarks of the 12 normal subjects (red) and 12 LQTS3 (green) cases. Q is zero at the starting point. The x-coordinates of landmarks were revised by Bazett correction. The abbreviations in the figure are defined in the main text of this paper. The 95% confidence intervals of the J point and TeEye are indicated by blue solid horizontal lines. The dashed ovals indicate the 95% confidence ellipses for the other landmarks. The corresponding 95% confidence ellipses for landmarks do not overlap with each other. The pale pink dots are the landmarks of normal subjects, and the pale green dots are landmarks of the patients with LQTS3.

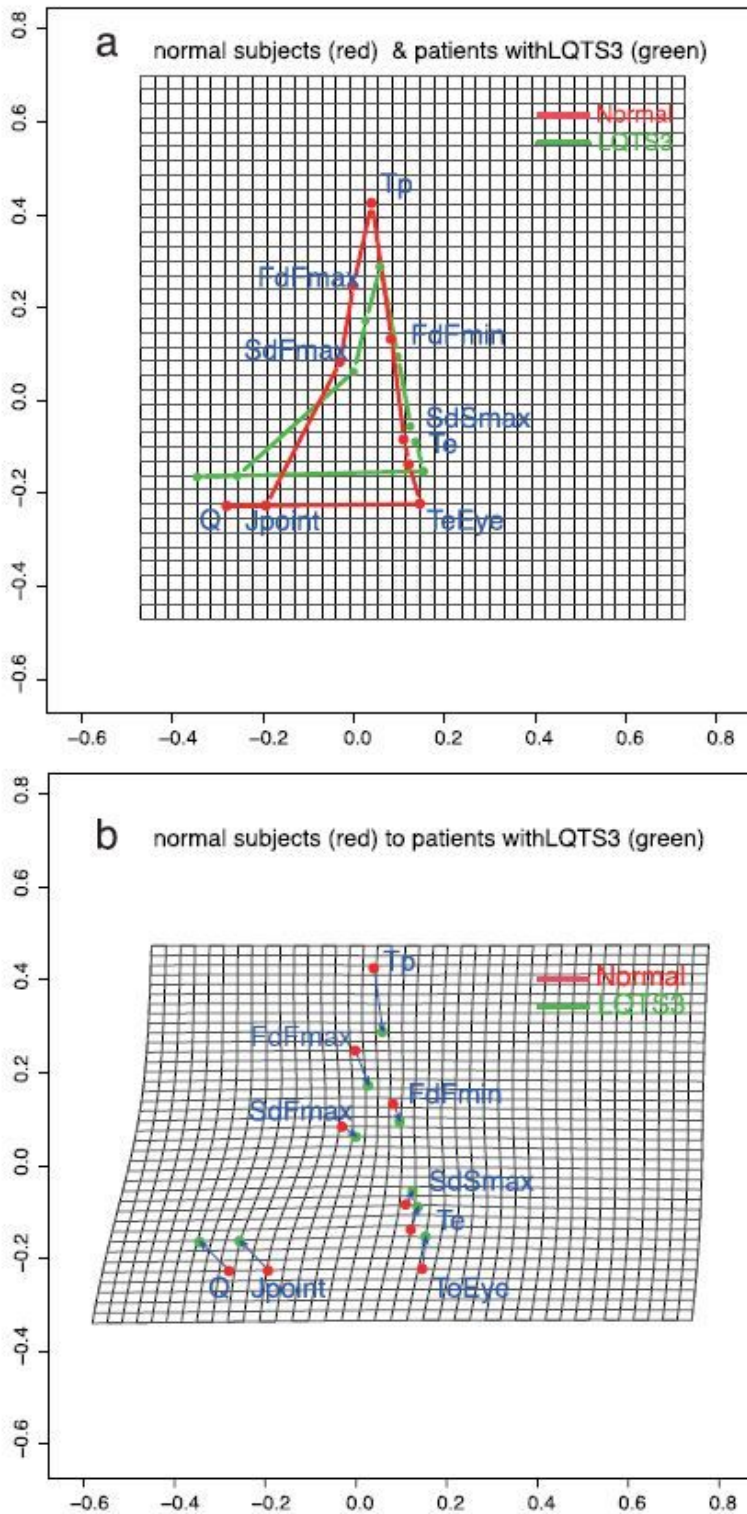


Figure 4

Panel a shows the mean shape of the T-wave in the normal subjects (red) and the mean shape of the T-wave in the patients with LQTS3 (green) by full GPA. Panel b shows thin-plate spline transformation grids to minimize the mixed energy from the normal mean shape (red) to the patients with LQTS3 mean shape (green), with blue arrows drawn from the normal subjects mean (red) to the patients with LQTS3 (green). The shape changes have not been magnified.

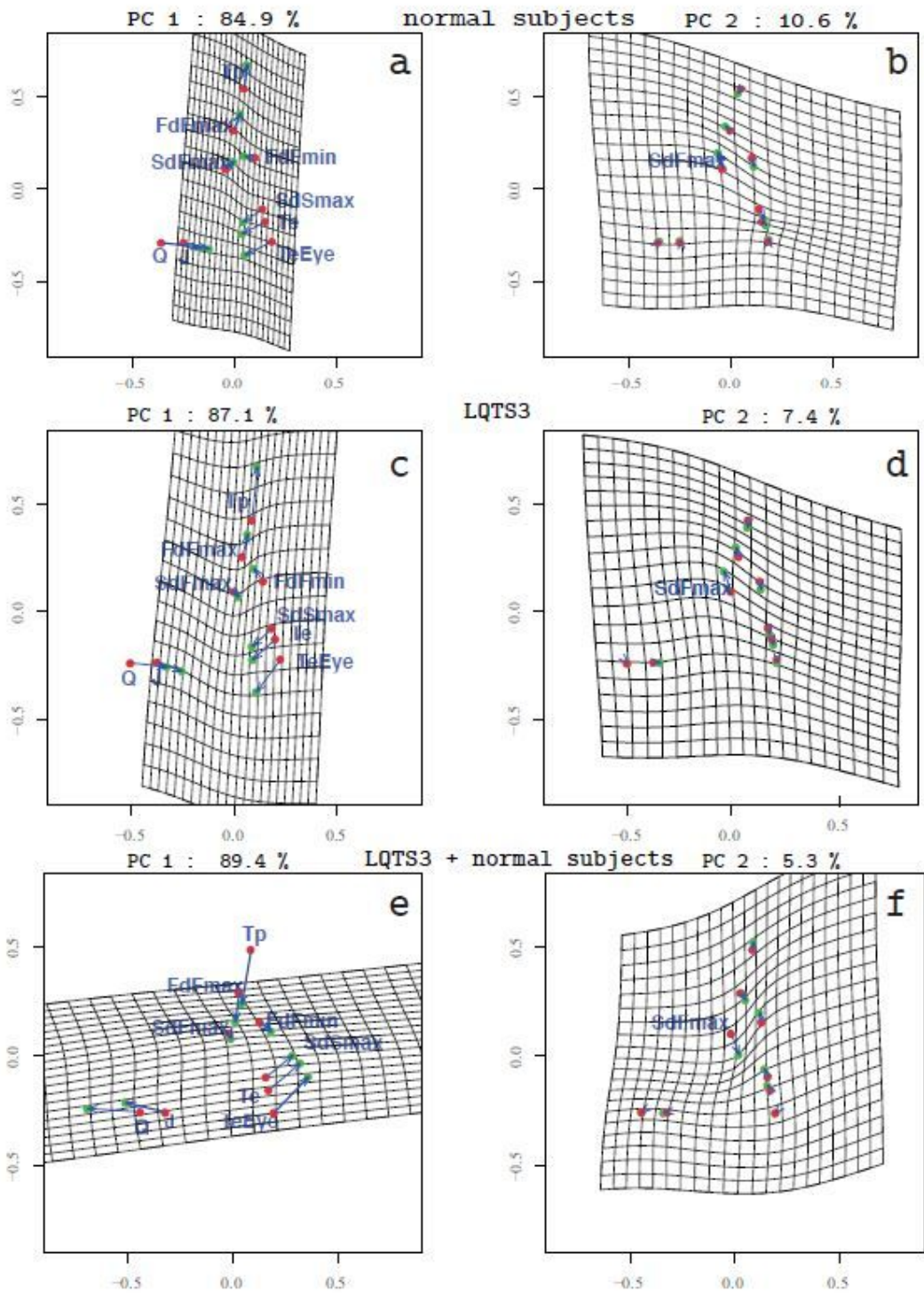


Figure 5

Changes in PC1 and PC2 in the normal subjects (panels a and b), patients with LQTS3 (panels c and d) and a combination of the two groups of subjects (panels e and f). A square grid is drawn on the mean shape (red points) and deformed using a pair of thin-plate splines to an icon (green points, mean+1 * standard deviation) along each PC (indicated by the blue vector from the mean to the icon). PC1 of the normal subjects (panel a) and PC1 of the patients of LQTS3 (panel c) show that Q, J, SdSmax, Te and TeEye

are attracted to the vertical center and narrowed. FdFmax and Tp are displaced upward. The SdFmax of PC2 of the normal subjects (panel b) and that of the patients with LQTS3 (panel d) is displaced to the upper left. In the case of the combination of the two types, PC1 (panel e) for the Procrustes mean shape shows the displacement to the left of Q and J. FdFmax and Tp were displaced downward. SdSmax, Te, and TeEye were pulled to the upper right. There are almost no changes in SdFmax and FdFmin. PC2(panel f) for the Procrustes mean shape shows the displacement of SdFmax to the lower right.

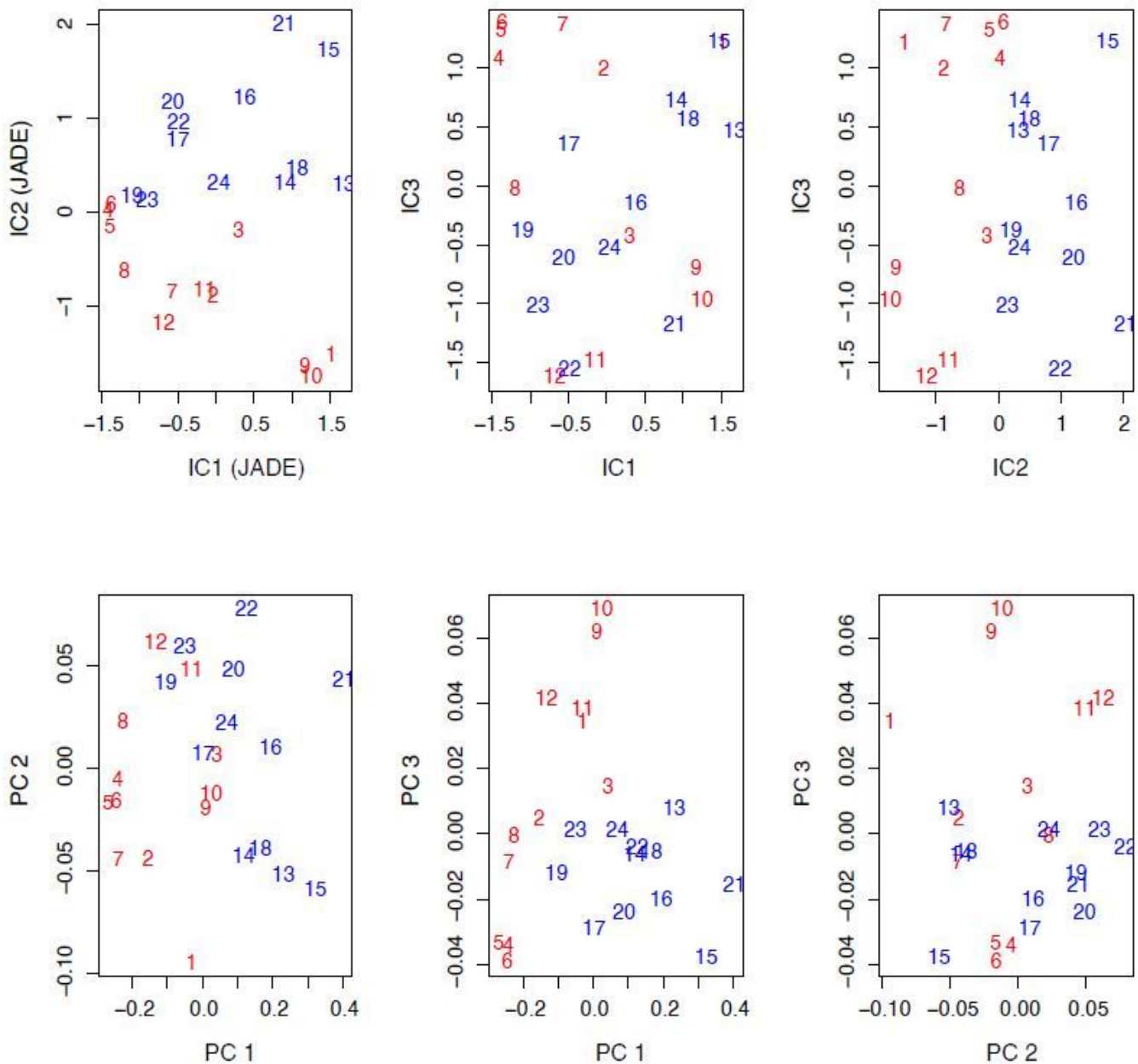


Figure 6

Plot of the first three IC scores(top row), and the first three PC scores (bottom row) for a combination of the landmark data. Red numbers indicate normal subjects, and blue numbers indicate patients with LQTS3. IC2 gives quite good separation between normal subjects and patients with LQTS3.